Cell Death and Differentiation (2006) 13, 1138–1146

www.nature.com/cdd

Regulation of osteoclast differentiation by the redox-dependent modulation of nuclear import of transcription factors

Y-J Huh[1,2,9,10], J-M Kim[1,2,9,10], H Kim[2,10], H Song[3], H So[4], SY Lee[5], SB Kwon[5], HJ Kim[6,9], H-H Kim[6,9], SH Lee[7], Y Choi[7], S-C Chung[8], D-w Jeong*[,9] and B-M Min*[,1,2,9]

[1] Department of Oral Biochemistry and Craniomaxillofacial Reconstructive Science, Dental Research Institute, Seoul National University College of Dentistry, Seoul 110-749, Korea
[2] IBEC, Seoul National University College of Dentistry, Seoul 110-749, Korea
[3] Department of Biological Sciences, Korea Advanced Institute of Science and Technology, Daejeon 305-701, Korea
[4] Vestibulorcochlear Research Center, Wonkwang University School of Medicine, Chonbuk, Ik-San 570-749, Korea
[5] Division of Molecular Life Sciences and the Center for Cell Signaling Research, Ewha Woman's University, Seoul 120-750, Korea
[6] Department of Cell and Developmental Biology, Seoul National University College of Dentistry, Seoul 110-749, Korea
[7] Department of Pathology and Laboratory Medicine, Abramson Cancer Research Institute, University of Pennsylvania, Philadelphia, PA, USA
[8] Department of Oral Medicine and Oral Diagnosis, Seoul National University College of Dentistry, Seoul 110-749, Korea
[9] BK21 HLS, Seoul National University, Seoul 110-749, Korea
[10] These authors contributed equally to this work.
* Corresponding authors: D-w Jeong, BK21 HLS, Seoul National University, 28 Yeonkun-Dong, Chongno-Ku, Seoul 110-749, Korea. Tel: +82-2-740-8664; Fax: +82-2-740-8665; E-mail: dwjeong@snu.ac.kr or B-M Min, Department of Oral Biochemistry and Craniomaxillofacial Reconstructive Science, Seoul National University College of Dentistry, 28 Yeonkun-Dong, Chongno-Ku, Seoul 110-749, Korea. Tel: +82-2-740-8661; Fax: +82-2-740-8665; E-mail: bmmin@snu.ac.kr

Received 28.12.04; revised 04.8.05; accepted 25.8.05; published online 14.10.05
Edited by A Finazzi-Agrò

Abstract

This study sought to characterize the reduced glutathione (GSH)/oxidized GSSG ratio during osteoclast differentiation and determine whether changes in the intracellular redox status regulate its differentiation through a RANKL-dependent signaling pathway. A progressive decrease of the GSH/GSSG ratio was observed during osteoclast differentiation, and the phenomenon was dependent on a decrease in total glutathione via downregulation of expression of the γ-glutamylcysteinyl synthetase modifier gene. Glutathione depletion by L-buthionine-(*S,R*)-sulfoximine (BSO) was found to inhibit osteoclastogenesis by blocking nuclear import of NF-κB and AP-1 in RANKL-propagated signaling and bone pit formation by increasing BSO concentrations in mature osteoclasts. Furthermore, intraperitoneal injection of BSO in mice resulted in an increase in bone density and a decrease of the number of osteoclasts in bone. Conversely, glutathione repletion with either *N*-acetylcysteine or GSH enhanced osteoclastogenesis. These findings indicate that redox status decreases during osteoclast differentiation and that this modification directly regulates RANKL-induced osteoclastogenesis.

Cell Death and Differentiation (2006) **13,** 1138–1146.
doi:10.1038/sj.cdd.4401793; published online 14 October 2005

Keywords: reactive oxygen species (ROS); redox status; GSH/GSSG ratio; osteoclastogenesis; RANKL-dependent signaling

Abbreviations: OCs, osteoclasts; OBs, osteoblasts; GSH, reduced glutathione; ROS, reactive oxygen species; RANKL, receptor activator of NF-κB ligand; ERK, extracellular signal-regulated kinase; JNK, c-Jun NH_2-terminal kinase; γ-GCS, γ-glutamylcysteinyl synthetase; TRAF, TNF receptor-associated factor; BMMs, bone marrow-derived monocytes; M-CSF, macrophage colony-stimulating factor; BSO, L-buthionine-[*S,R*]-sulfoximine; NAC, *N*-acetylcysteine; TRAP, tartrate-resistant acid phosphatase; TRAP(+) MNCs, tartrate-resistant acid phosphatase-positive multinuclear cells; MAPKs, mitogen-activated protein kinases; EMSA, electrophoretic mobility shift assay; DTNB, 5,5′-dithiobis-(2-nitrobenzoic acid); RT-PCR, reverse transcription-polymerase chain reaction; HPRT, hypoxanthine-guanine phosphoribosyltransferase; OVXs, ovariectomies; DMEM, Dulbecco's modified Eagle's medium; FBS, fetal bovine serum; α-MEM, minimum essential medium-alpha

Introduction

Redox status has been implicated in numerous pathological processes, including aging, alcoholism, cancer, cirrhosis, diabetes, neurodegenerative diseases, and viral infections.[1–3] It is further known that most aging and developing cells display redox shifts toward oxidizing environments[4] and that these changes in redox status regulate cellular development (proliferation, differentiation, and apoptosis) through signal transduction, enzymatic activity, cell cycle alterations, and protein synthesis and folding.[5]

The balance between oxidants and antioxidants, and the ratio of reduced glutathione (GSH) to oxidized GSSG in particular, has been used to measure cellular redox status. Using glutathione levels in this way is appropriate because this antioxidant is a major determinant of redox status in aerobic organisms and has been shown to act in several vital functions.[6,7] Glutathione scavenges reactive oxygen species (ROS) and electrophiles and serves as an antioxidant enzyme cofactor. This antioxidant also maintains thiol groups essential to protein function and cellular cysteine levels. Finally, glutathione modulates proper protein folding in the endoplasmic reticulum.

Several studies have recently linked ROS to bone metabolism.[8–11] Additionally, bone remodeling is known to come about through the opposing actions of bone-forming osteoblasts (OBs) and bone-resorbing osteoclasts (OCs).

Multinuclear OCs are derived from the monocyte-macrophage lineage of hematopoietic progenitor cells through a multistep process of cell adhesion, proliferation, motility, cell–cell contact, and terminal fusion to form the multinucleated giant cells.[12,13] The process is initiated by binding of the receptor activator of NF-κB ligand (RANKL; also called TNF-related activation-induced cytokine, TRANCE) to its receptor (RANK; also called TRANCE receptor) and subsequently propagates by activation of several signaling cascades.[14] The activated signaling pathways include NF-κB, extracellular signal-regulated kinase (ERK), c-Jun NH_2-terminal kinase (JNK), and p38 mitogen-activated protein kinase through recruitment of the TNF receptor-associated factors (TRAFs). These signaling events are intimately involved in the regulation of OC differentiation and function.[15] Once OCs have differentiated, their resorption of bone could be facilitated by ROS generated by NADPH oxidase. Inhibition of NADPH oxidase led to reductions of ROS and bone resorption.[11] These results are consistent with the theory that ROS generation in OCs is dependent on NADPH oxidase activity and directly related to OC function.

From the reports outlined above, we have postulated that the cellular GSH/GSSG ratio may alter during OC differentiation and that the accompanying changes in redox status may influence OC differentiation. It is reported here that the GSH/GSSG ratio indeed decreased in a time-dependent fashion during OC differentiation and that its differentiation could be modulated by changing the cellular redox status through glutathione-depletion or glutathione-repletion. Most significantly, regulation of OC differentiation by cellular redox status was achieved by orchestrating the nuclear import of cytosolic transcription factors such as NF-κB and AP-1.

Results and discussion

Decrease of GSH/GSSG ratio during OC differentiation

Several studies have reported that redox status generally decreases during cellular development; this study targeted redox status changes specifically during OC differentiation. To that end, murine macrophage RAW264.7 cells and bone marrow-derived monocytes (BMMs) were differentiated into OCs in the presence of RANKL and macrophage colony-stimulating factor (M-CSF) plus RANKL, respectively. Differentiation of both cell types was associated with a time-dependent decrease in the GSH/GSSG ratio (Figure 1a and d). Theoretically, the ratio would be altered by changes in either total glutathione (GSH + GSSG) or GSSG contents; in this study, however, changes in redox status during OC differentiation were dependent on total glutathione contents (Figure 1b and e). A change in the total cellular glutathione

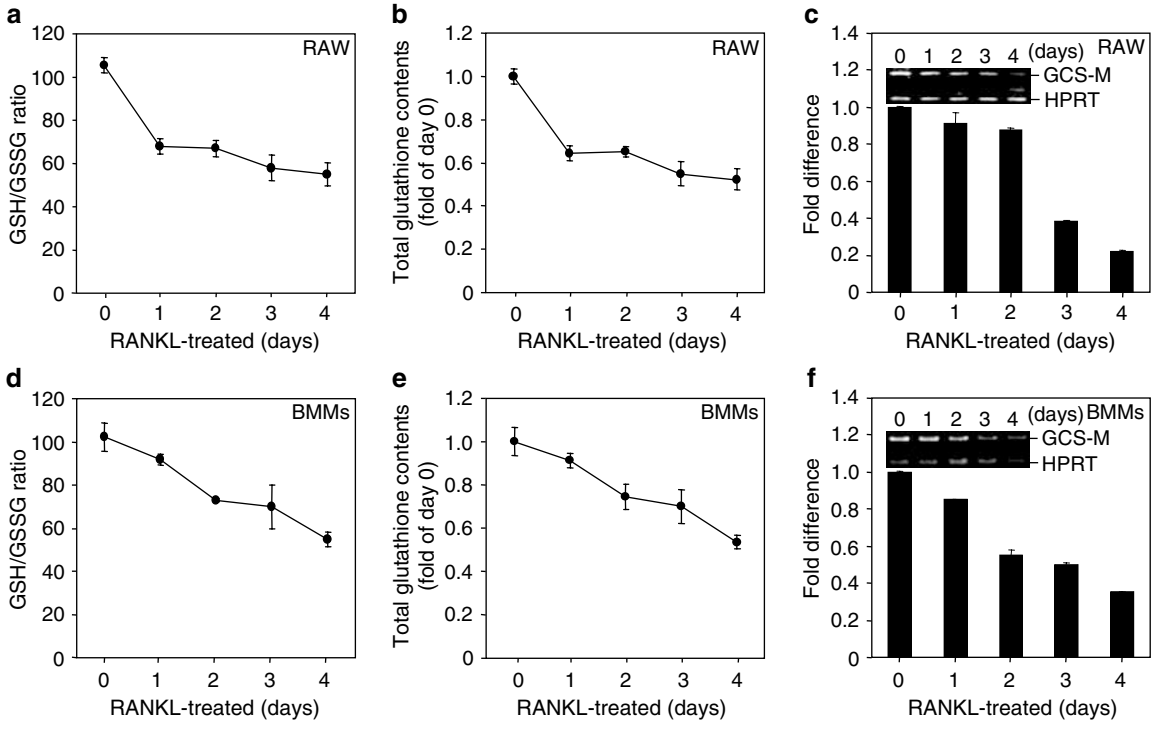

Figure 1 Glutathione status during OC differentiation. (**a**) GSH/GSSG ratio change and (**b**) total glutathione (GSH + GSSG) level during OC differentiation from RAW264.7 cells. Cells were collected at 1-day intervals for 4 days after RANKL-induced OC differentiation. The GSH/GSSG ratio and total glutathione content were measured in these cells' cytosolic fractions. (**c**) Measurement of GCS-M mRNA level by real-time PCR during OC differentiation from RAW264.7 cells. GCS-M mRNA quantification was determined by RT-PCR (insets) and real-time PCR. Insets: The expected fragment sizes were 449 bp for GCS-M and 177 bp for HPRT. Data are expressed as mean $\pm$ S.D. ($n = 3$). (**d**) GSH/GSSG ratio change and (**e**) total glutathione level during OC differentiation from BMMs. OC precursors derived from BMMs of C57BL/6 mice were cultured in media containing M-CSF and RANKL for 4 days with collection at 1-day intervals. (**f**) Measurement of GCS-M mRNA level by real-time PCR during OC differentiation from BMMs. The assay conditions were the same as those in (**c**). Data are expressed as mean $\pm$ S.D. ($n = 3$)

level could be effected by diverse cellular actions,[6,7] including glutathione synthesis by γ-glutamylcysteinyl synthetase (γ-GCS), a glutathione synthesis rate-limiting enzyme; export of cellular GSSG by a transporter; and degradation of extracellular GSSG by γ-glutamyltranspeptidase. This study examined modulation of γ-GCS expression during OC differentiation in an effort to explain the observed gradual decrease in total glutathione.

γ-GCS is a heterodimeric enzyme composed of catalytic (GCS-C) and modifier subunits (GCS-M).[16] Regulation of expression of the modifier subunit gene is known to principally control the activities of both γ-GCS subunits. In the present study, the GCS-M mRNA level was observed to be downregulated during OC differentiation using a reverse transcription-polymerase chain reaction (RT-PCR) (Figure 1c and f, insets) and real-time PCR. Taken together, these data indicate that the decrease in the GSH/GSSG ratio during OC differentiation was caused by downregulation of the GCS-M gene involved in glutathione synthesis.

Effects of an oxidizing or reducing cellular redox status on OC differentiation

Herein, OCs were observed to undergo redox shifts toward more oxidizing environments during their differentiation. Previous reports suggest that ROS, such as hydrogen peroxide and superoxide, enhance bone resorption[8,9] and that the partial depletion of glutathione brought on by treatment with a small amount of L-buthionine-(*S,R*)-sulfoximine (BSO, 10 μM), a specific inhibitor of γ-GCS, stimulates RANKL-induced OC differentiation.[17] These results suggest that the severe depletion and adequate repletion of glutathione at the period of RANKL-induced glutathione reduction could have an effect on OC differentiation. It was thus speculated that a perturbation in redox status could result in mis-regulation of OC differentiation. Several redox modifiers were employed to test this hypothesis. Reduced GSH; BSO; and *N*-acetylcysteine (NAC), a glutathione precursor, were all introduced prior to RANKL-induced OC differentiation. It was discovered that intracellular glutathione levels could be modulated by adjusting the exposure time and concentration of the redox modifier used.

With a 15-h pretreatment with 300 μM BSO, total glutathione contents in RAW264.7 cells declined from 101.51 ± 12.84 to 10.14 ± 2.08 nmol/mg of protein. While glutathione depletion by BSO inhibited formation of tartrate-resistant acid phosphatase-positive multinuclear cells (TRAP(+) MNCs), glutathione repletion by NAC or GSH increased the number of TRAP(+) MNCs (Figure 2) and TRAP activity (data not shown) compared with a RANKL-only control.

Cell growth is vital to OC differentiation,[18] so the influence of redox modifiers on cell growth was also evaluated. None of the redox modifiers themselves introduced during OC differentiation had any effect on cell viability. This was determined using the trypan blue exclusion method and a colorimetric MTT-based assay (data not shown). The suppressive or stimulatory effects of a redox modifier on OC differentiation do not appear, therefore, to be related to

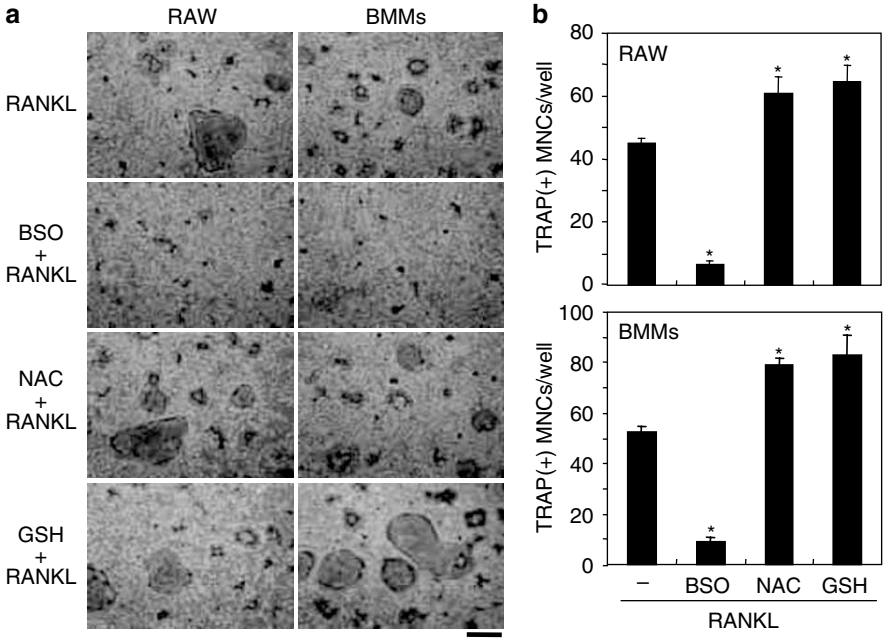

Figure 2 The effects of endogenous glutathione modification on OC differentiation. (**a**) Photographs and (**b**) the number of TRAP-positive OC-like cells. RAW264.7 cells (2×10^3 cells/well) and BMMs (1×10^4 cells/well) were seeded on a 96-well culture plate; pretreated for 15 h with BSO (300 μM), NAC (4 mM), or GSH (4 mM); and then treated for 4 days with RANKL (RAW264.7 cells) or M-CSF plus RANKL (BMMs). Cells were washed with PBS, fixed, and stained for TRAP after differentiation into OCs. Stained cells were photographed, and TRAP(+) MNCs containing three or more nuclei were counted as OCs. Data are expressed as mean $\pm$ S.D. ($n = 3$). *$P < 0.01$ *versus* RANKL alone. Bar, 100 μm

differences in cell viability. Taken together, these observations indicate that OC differentiation can be regulated through redox-dependent mechanisms.

Correlation of redox status and cellular signaling in OC differentiation

A growing body of studies reports that RANKL-induced OC differentiation relies on a signal by a TRAF by way of downstream signal activations such as mitogen-activated protein kinases (MAPKs) and NF-κB. In examining whether RANKL-dependent signaling could be regulated by redox status, redox modifiers were found to have no effect on MAPK (ERK, JNK, and p38) signaling or IkBα degradation from an NF-κB/IκB complex (Figure 3a). When an NF-κB- or AP-1-dependent luciferase reporter plasmid was transfected into RAW264.7 cells and stimulated with RANKL in the presence of BSO, NAC, or GSH, luciferase activity varied according to redox status. While luciferase activity of the RANKL-stimulated cells in the presence of BSO was similar to that of the untreated control (Figure 3b, column 3), the activity of the RANKL-stimulated cells in the presence of NAC or GSH was significantly higher than that of the RANKL-only cells (Figure 3b, columns 4 and 5). These results were confirmed by electrophoretic mobility shift assay (EMSA) analysis showing that BSO resulted in a decrease of NF-κB and AP-1 DNA binding affinity in nuclear extracts (Figure 3c).

The observed events could be caused by three cellular mechanisms: (i) a more oxidizing environment created by the presence of BSO could inhibit NF-κB and AP-1 gene expression, (ii) a low redox status could decrease nuclear import of transcription factors, or (iii) oxidized and/or misfolded transcription factors in a less reduced state could exhibit low DNA-binding affinity. Immunoblot analysis was performed to verify or disprove these possible mechanisms. The expression of p65 for NF-κB and of c-Jun for AP-1 was found to be identical in whole-cell lysates (Figure 4a). This suggests that the activities of these transcription factors were unrelated to their levels of expression in the cell. Additionally, Figure 3a suggests that NF-κB activities had no connection to the release of activated NF-κB from the NF-κB/IκB complex. Despite these findings, the possibility that intracellular redox status may be important to nuclear translocation of these transcription factors cannot be excluded. As a result of this potential regulatory role, the present study also examined redox-dependent mechanisms of modulating subcellular localization of transcription factors. Subcellular fractionation (Figure 4b) and confocal microscopic analysis (Figure 4c) revealed that nuclear translocation of NF-κB and AP-1 by RANKL was inhibited by preincubation with BSO. These findings indicate that nuclear translocation of the transcription factors during osteoclastogenesis could be regulated by cellular redox status. Consistent with this study's results, numerous reports have placed nuclear localization of a variety

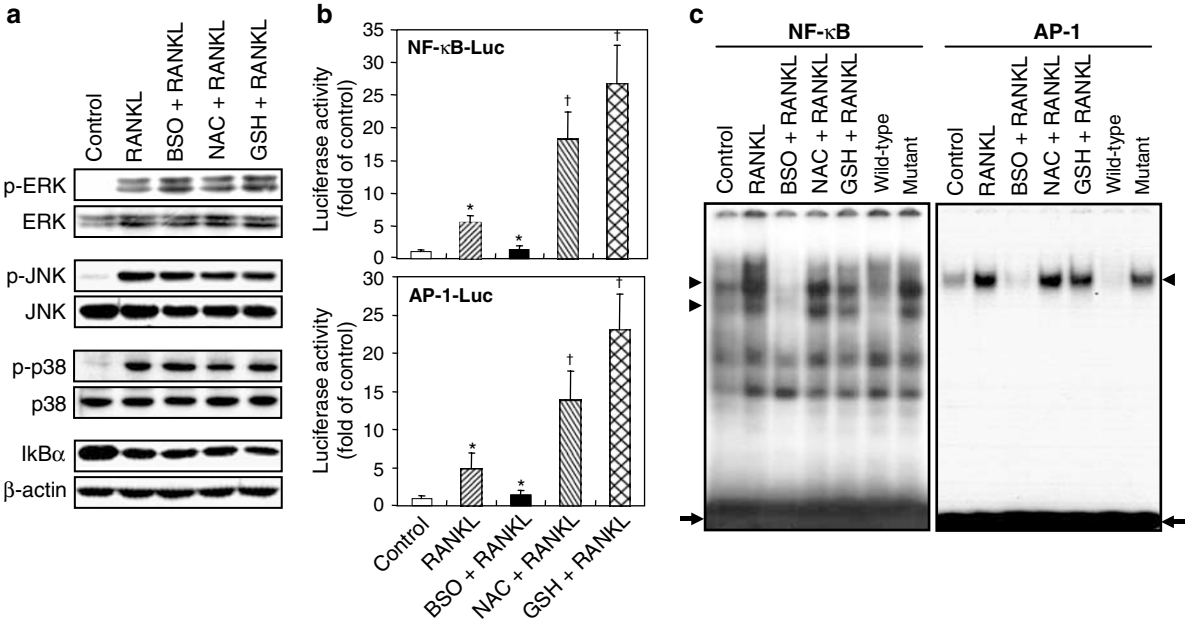

Figure 3 Changes in RANKL-induced signaling for differing redox status. (**a**) Immunoblot analysis. RAW264.7 cells (2×10^5 cells/60-mm dish) were pretreated with BSO, NAC, and GSH for 2 days and then stimulated with RANKL for 20 min. Cytosolic fractions (25 μg/lane) were subjected to immunoblot analysis for detection of p-ERK, ERK, p-JNK, JNK, p-p38, p38, IκBα, and β-actin. (**b**) Luciferase reporter assay. NF-κB- or AP-1-dependent reporter plasmids were transfected into RAW264.7 cells (2×10^4 cells/well), whose selected ones were then treated with either BSO, NAC, or GSH for 2 days, and the remaining cells untreated. Cells, excluding control cells, were then stimulated with RANKL for one additional day and lysed, and assayed for luciferase activity as described in 'Materials and Methods'. $^*P<0.01$ *versus* RANKL-untreated control. $^\dagger P<0.05$ *versus* RANKL alone. (**c**) EMSA analysis. RAW264.7 cells (1×10^6 cells/100-mm dish) were treated as described in (**a**). Nuclear extracts were prepared and subjected to EMSA analysis for determination of the DNA-binding activities of NF-κB and AP-1. To access specific binding, nuclear extracts shown in lane 2 were subjected to EMSA analysis with prior incubation in 100-fold molar excess of unlabeled wild-type or mutant oligonucleotides for NF-κB or AP-1. The arrow and arrowhead indicate the free probe and the specific DNA-probe/transcription factor complex (NF-κB or AP-1), respectively. Results are representative of at least three independent experiments

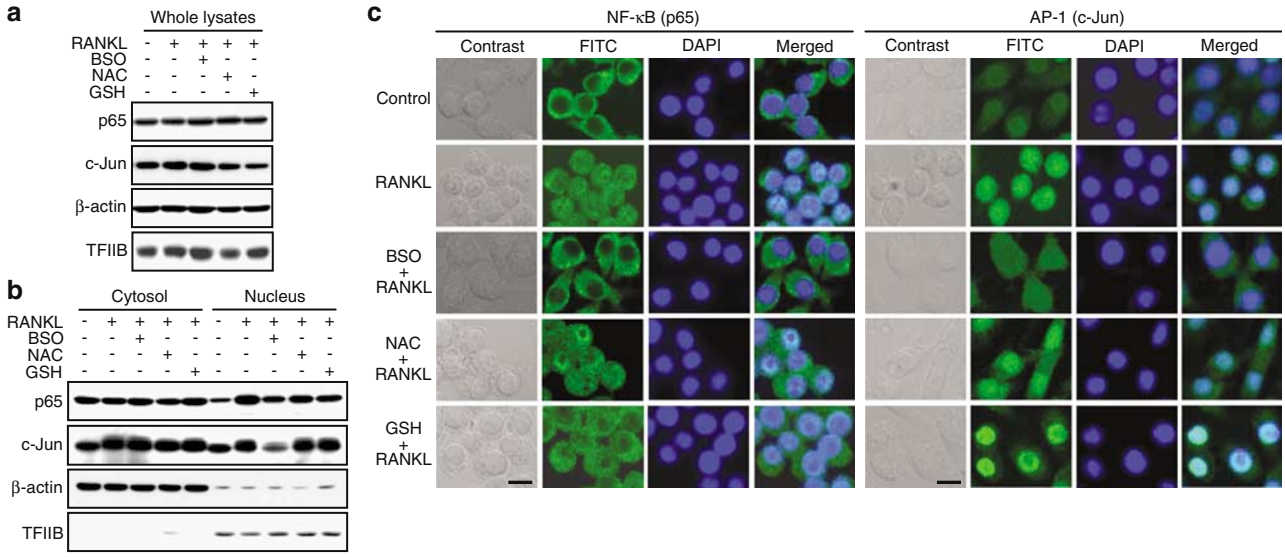

Figure 4 Inhibition of nuclear import of transcription factors by glutathione depletion. (**a**) Immunoblot analysis for p65 and c-Jun in whole lysates. After cells were treated as described in Figure 3a, whole-cell lysates were prepared and subjected to immunoblot analysis using a specific antibody to p65, c-Jun, β-actin, or TFIIB to confirm consistent application of nuclear extracts. Transcription factor distribution was characterized by immunoblot analysis of subcellular fractions (**b**) and confocal microscopy (**c**). Bar, 25 μm

of transcription factors under strict controlle of cellular redox status.[19–21] Changes in nuclear translocation of these transcription factors could be regulated by extent of imports to nucleus and exports from nucleus and the retention time in nucleus. Although the precise mechanisms of translocation of nuclear transcription factors are currently unclear, it could be associated with differences in culture conditions and/or cell types.

Inhibitory effect of combined RANKL and BSO on cell growth

Previous studies reported that endogenously generated and exogenously treated oxidative stress can induce a cell phase transition from a quiescent to a proliferative or apoptotic state.[22] These findings were tested here by quantifying free thiol groups in the cytosolic fractions (Figure 5a) and correlating these data with cell growth pattern (trypan blue exclusion method; Figure 5b) and flow cytometer analysis (propidium iodide staining; data not shown). While treatment with RANKL alone did not affect cell growth, RANKL-only treatment did induce intracellular peroxide accumulation (data not shown) and thus a decrease in redox status compared with the control (Figure 5a, column 2).

Treatment with BSO was also observed to decrease redox status, but it did not affect cell growth (Figure 5a and b, column 3). It was theorized that redox status would be yet further decreased by a combination of BSO and RANKL compared with either compound alone. In fact, BSO-mediated glutathione depletion displayed significantly increased cell susceptibility to RANKL-generated ROS (Figure 5b, column 4) and resulted in retarded cell growth (G2/M arrest, data not shown). In contrast, RANKL treatment in the presence of NAC or GSH maintained a higher redox status than with RANKL alone (Figure 5a, columns 5 and 6) and increased the formation of RANKL-induced TRAP(+) MNCs (Figure 2). Taken together, these results suggest that a higher redox status leads to increased OC differentiation and formation.

Inhibition of bone-resorbing activity in BSO-treated mature OCs and reduction of the number of OCs in BSO-treated mice

We investigated whether BSO can regulate bone-resorbing activity. When mature OCs were cultured on an OAAS plate coated with carbonated calcium phosphate, pit formation was gradually decreased by BSO in a dose-dependent manner (Figure 6a). This study then examined the effects of BSO on bone mineral density *in vivo*. When BSO (8 mmol/kg) was injected intraperitoneally into C57BL/6 mice at 4-day intervals for 4 weeks, the total and trabecular bone densities were significantly increased when compared with the PBS-administered mice (Table 1 and Figure 6b). To analyze the effects of BSO on bone loss *in vivo*, the mice were subjected to ovariectomies (OVXs). An increase in bone density by BSO was associated with a decrease in the number of OCs (Figure 6c). However, no significant difference of OB formation was seen in either BSO or OVX, or in both (Figure 6d). BSO-administered mice were normal in appearance with a body size similar to naïve mice, and the BSO had no effect on body weight. These findings suggest that cellular redox status can regulate both bone resorption and OC formation.

Regulation of OC differentiation plays an important role in maintaining bone homeostasis and contributes to understanding pathogenesis and therapy of bone diseases such as osteoporosis and osteopetrosis. Recent reports implicate OC-generated superoxide derived from NADPH oxidase in

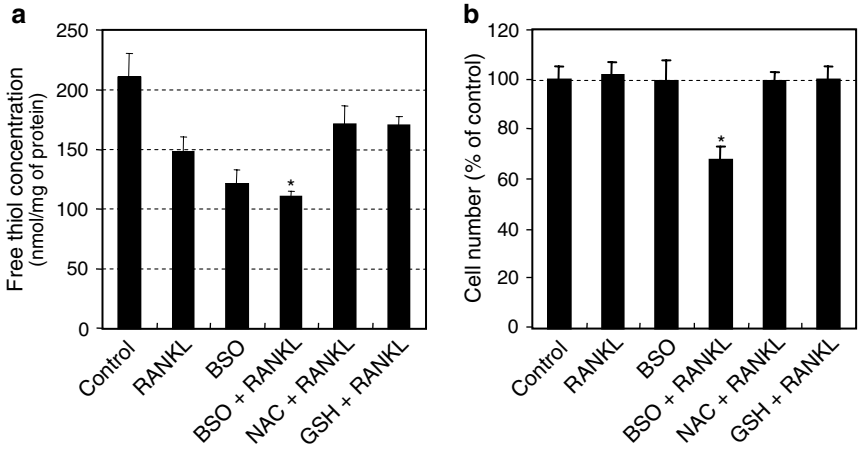

Figure 5 The effects of combined BSO and RANKL treatment on cell growth and cellular redox status. (**a**) Free thiol group content. RAW264.7 cells (2×10^5 cells/60-mm dish) were seeded; pretreated for 15 h with BSO, NAC, and GSH; and then treated for 2 days with RANKL. Cytosolic extracts were prepared and assayed for free thiol groups with DTNB. (**b**) Cell viability. After RAW264.7 cells were treated as described in (**a**), cells excluding trypan blue were counted after detachment by trypsinization. Data are expressed as percentages of the value for untreated cells (mean $\pm$ S.D., $n=3$). *$P<0.01$ *versus* RANKL alone

Table 1 Increase in the bone mineral density of mice administered by BSO

Total bone density		Trabecular bone density	
Control	**BSO**	**Control**	**BSO**
389.71 $\pm$ 11.33 (F)	402.82 $\pm$ 5.27 (F)*	215.55 $\pm$ 9.09 (F)	230.30 $\pm$ 6.10 (F)*
342.57 $\pm$ 4.93 (M)	356.96 $\pm$ 7.27 (M)*	243.39 $\pm$ 9.06 (M)	265.71 $\pm$ 8.44 (M)†

BSO (8 mmol/kg) was administered by intraperitoneal injection of C57BL/6 mice (4-week old, $n=7$ in each group) at 4-day intervals for 4 weeks to examine BSO effects on bone density. Bone mineral density (mg/cm^2) of the tibia was analyzed with pQCT by XCT research SA (STRATEC). *$P<0.05$ *versus* control. $^{\dagger}P<0.01$ *versus* control. M, male; F, female

OC formation and bone resorption.[8,9,11,17] Overexpression of catalase[10] and treatment with DPI,[11] a specific NADPH oxidase inhibitor, have indeed been shown to decrease superoxide production in OCs and block OC formation and bone resorption. In addition, it has been reported that a small amount of H_2O_2 (1 μM) and a partial depletion of the intracellular glutathione pool by BSO (10 μM) enhance RANKL-induced OC differentiation via NF-κB activation.[17]

It is well known that ROS are linked with cellular signaling as second messengers.[23,24] Thus, transient elevation of endogenously generated ROS and an appropriate amount of exogenously treated ROS are essential to mediating signal transduction. Together, these previous reports indicate that various oxidative stresses are responsible for cellular transcription factor activation.

In the present study, it was observed that severe glutathione depletion by BSO (300 μM) inhibited RANKL-mediated OC differentiation by blocking nuclear import of the cellular transcription factors. This suggests that transcription factor action in RANKL-mediated signaling could be positively or negatively controlled by cellular redox status. Thus, moderate and severe oxidative stress could act as dual functions in osteoclastogenesis. Opposing effects as mentioned above may result from fluctuating redox status, which itself depends on time and concentration of oxidant exposure. Fundamentally, this study suggests that functional activities of the transcription factors investigated, including nuclear import, were precisely controlled by cellular redox status.

Several studies have sought to identify molecular targets for the prevention of pathological bone resorption. Recently, selective blocking of NF-κB, including deletion of specific NF-κB family subunits;[25] inhibition of the IKK complex by the NF-κB essential modulator-binding domain;[26] and overexpression of dominant-negative IκBα,[27] has been shown to inhibit RANKL-induced OC differentiation and bone loss *in vivo*. Among others, we here have put forth NF-κB and AP-1, both dependent on redox-signaling via RANKL-mediated OC differentiation, as promising targets for bone disease therapy.

The findings of this study demonstrate that (i) a decrease in the GSH/GSSG ratio and an accumulation of ROS during osteoclastogenesis led to this reduction in redox status; (ii) glutathione depletion by BSO blocked OC differentiation by inhibiting the nuclear import of transcription factors related to RANKL-dependent signaling and bone-resorbing activity in mature OCs; (iii) intraperitoneal injections of BSO in mice resulted in increased bone density and decreased OC formation in the bone. Conversely, glutathione repletion with NAC or GSH *in vitro* enhanced OC formation by RANKL. Taken together, our results indicate that a redox shift toward a more oxidizing environment during OC differentiation is important to its differentiation and bone remodeling. ROS transiently generated by RANKL activate transcription factors NF-κB and AP-1 at early stages of differentiation and induce differentiation-linked gene expression. A lowered redox status in subsequent stages, resulting from accumulation of RANKL-generated ROS and decreased glutathione synthesis, may

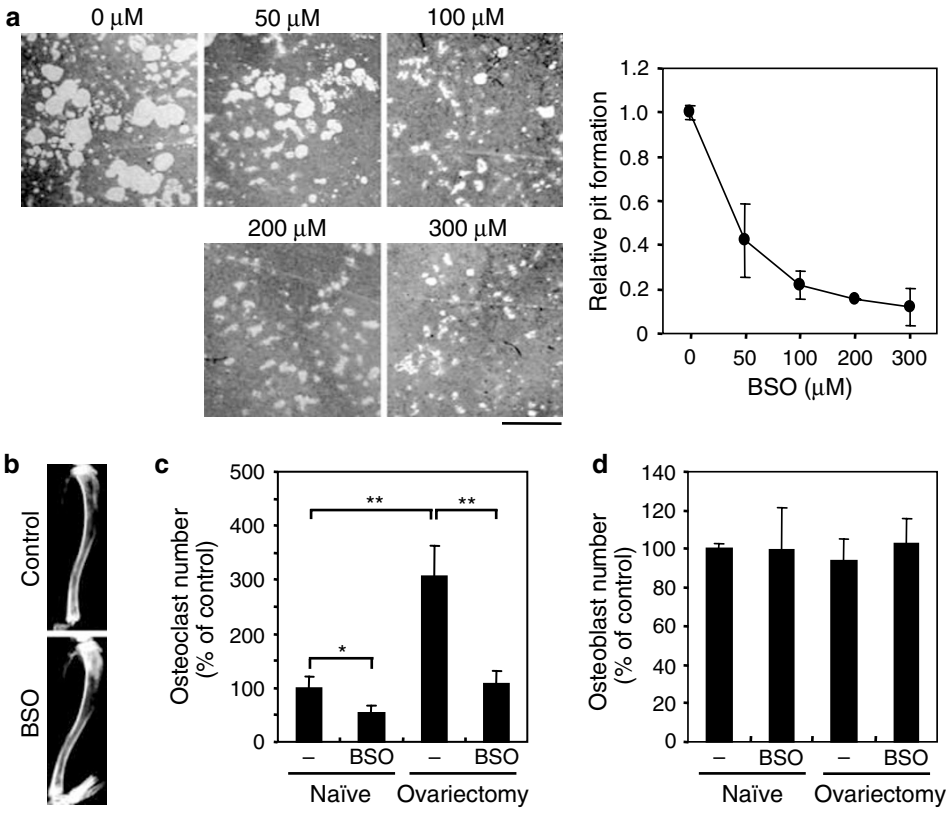

Figure 6 Assessment of the effect of BSO on bone resorption and density. (**a**) Inhibition of bone resorption by BSO. After mature OC formation on OAAS plates, cells were treated with BSO (0–300 μM) and cultured for an additional 2 days. The pit area was analyzed as described in the Materials and Methods section. Data are expressed as mean $\pm$ S.D. ($n=3$). Bar, 1 mm. (**b**) Bone density by BSO in mice. Naïve mice were injected intraperitoneally with or without BSO (8 mmol/kg) at 4-day intervals for 4 weeks. Bone from the tibia was X-rayed using of a SOFTEX CMB-2 (SOFTEX, Japan). (**c**) Inhibitory effect of BSO on naïve or OVX-induced OC formation in mice. After microscope sections (4 μm) of tibia from mice treated as described in (**b**), bone tissue was subjected to histological analysis by staining with TRAP to detect OC formation. Data are expressed as percentages of the value for BSO-untreated naïve mice (mean $\pm$ S.D., $n=4$). $^*P<0.05$. $^{**}P<0.01$. (**d**) Effect of BSO on naïve or OVX-induced OB formation in mice. OB formation was analyzed using hematoxylin–eosin staining. Data are expressed as percentages of the value for BSO-untreated naïve mice (mean $\pm$ S.D., $n=4$)

delay RANKL-induced OC differentiation because nuclear import of transcription factors is inhibited. We reported here that there is indeed a close relationship between redox status and OC differentiation.

Materials and Methods

Cell cultures

Prior to OC differentiation, the murine monocytic RAW264. 7 cell line that can differentiate into OC-like cells in the presence of RANKL was maintained under a humidified atmosphere of 5% CO_2 at 37°C in Dulbecco's modified Eagle's medium (DMEM; Invitrogen) supplemented with antibiotics and 10% fetal bovine serum (FBS).

OC differentiation

OC differentiation from BMMs was achieved as reported by Wani *et al.*[28] Briefly, BMMs were isolated from the tibia and femur of 6-week-old C57BL/6 female mice by flushing the bone marrow cavity with minimum essential medium-alpha (α-MEM; Invitrogen). The cells were then centrifuged, exposed to hypotonic ACK buffer (0.15 mM NH_4Cl, 1 mM KCO_3, and 0.1 mM EDTA, pH 7.4) at room temperature for 30 s to remove red blood cells,[29] and incubated with α-MEM containing M-CSF (5 ng/ml, Genetics Institute) for 12 h to separate adherent and nonadherent cells. Nonadherent cells were collected, suspended in α-MEM containing antibiotics and 10% FBS, counted, seeded on a 60-mm culture dish at 1×10^6 cells/dish, and cultured in α-MEM containing M-CSF (30 ng/ml) for 2 days to generate OC precursors. Floating cells were removed from the culture by aspiration and further incubated with media containing M-CSF (30 ng/ml) and RANKL (300 ng/ml) for 4 days to allow differentiation of these precursors into OCs. Fresh media was applied at day 3. RAW264.7 cells were differentiated into OCs by a similar process: cells were cultured (2×10^5 cells/60-mm dish) in α-MEM containing RANKL (300 ng/ml), fresh media containing RANKL was applied after 3 days, and the cells were incubated for an additional 24 h.

Measurement of GSH/GSSG ratio

After RAW264.7. cells were cultured with RANKL and OC precursors with M-CSF and RANKL, cells were harvested at 1-day intervals for 4 days and stored at -70°C until use. The GSH/GSSG ratio was measured with the glutathione reductase/5,5′-dithiobis-(2-nitrobenzoic acid) (DTNB) recycling assay kit (BIOXYTECH® GSH-412™ OXIS International) under the conditions recommended by the manufacturer. Total glutathione and

GSSG contents were analyzed from GSH and GSSG standard curves. Concentrations were converted to nmol/mg of protein, and reduced GSH concentrations were found by subtracting GSSG from total glutathione. Finally, the GSH/GSSG ratio was calculated by dividing the difference between total glutathione and GSSG concentrations by the GSSG concentration (ratio = ((total glutathione)−2(GSSG))/(GSSG)).

RT-PCR and real-time quantitative PCR

GCS-M mRNA levels were determined by RT-PCR. Total RNA was reverse transcribed to cDNA, which allowed for PCR amplification of GCS-M and hypoxanthine-guanine phosphoribosyltransferase (HPRT) (30 cycles of denaturation at 94°C for 1 min, annealing at 57°C for 30 s, and extension at 72°C for 1 min). The GCS-M primers were designed from the catalogued sequence for this gene: 5′-CATGCAGTGGAGAAG-3′ and 5′-CTTGCCTCAGAGAGC-3′. HPRT primers for normalization of the expression level were also prepared: 5′-GTAATGATCAGTCAACGGGG GAC-3′ and 5′-CCAGCAAGCTTGCAACCTTAACCA-3′. Also, real-time RT-PCR was carried out using the 7500 Real-time PCR System (Applied Biosystems). GCS-M (GenBank accession no. NM_008129) and HPRT (GenBank accession no. NM_013556) primers were designed as follows: forward for GCS-M, 5′-CAGTTGGAGCAGCTGTATCAGT-3′; reverse for GCS-M, 5′-TTGTTTAGCAAAGGCAGTCAAA-3′; forward for HPRT, 5′-CCTAAGATGAGCGCAAGTTGAA-3′; reverse for HPRT, 5′-CCACAG GACTAGAACACCTGCTAA-3′. The cDNA was prepared using reverse transcriptase (Invitrogen) and a random hexamer, and then subjected to real-time PCR amplification using SYBR® Green PCR Master Mix (Applied Biosystems). This contained a 300 nM final concentration of each primer and cDNA, corresponding to 100 ng of total RNA. After incubation at 50°C for 2 min and 95°C for 10 min, the PCR cycling was as follows: 40 cycles at 95°C for 15 s and 60°C for 1 min. To analyze the data, cycle threshold values were determined by automated threshold analysis with Sequenced Detection Software version 1.3, after which the calculated cycle threshold values were exported to Microsoft Excel for analysis. The relative expression of GCS-M mRNA was calculated using the comparative cycle threshold method according to the manufacturer's procedures (Applied Biosystems).

Luciferase reporter assay

RAW264.7. cells were suspended in DMEM containing 10% FBS, seeded on 24-well culture plates at 2×10^4 cells/well, and adapted for 12 h. Cells were incubated for 1 h with a total of 2 μg of plasmid (1 μg of NF-κB- or AP-1-dependent luciferase reporter and 1 μg of pcDNA3-β-gal), 6 μl of Tfx™-50 reagent (Promega), and 200 μl of serum-free α-MEM. In all, 800 μl of α-MEM containing FBS was then added and incubation continued. After 6-h incubation, cells were treated with redox modifiers (300 μM BSO, 4 mM NAC, and 4 mM GSH) for 2 days and stimulated with RANKL. Luciferase activity was determined after 24-h of RANKL treatment, using a Bright-Glo™ luciferase assay system (Promega) and a luminometer (Turner Designs Instrument), and then normalized with respect to β-galactosidase activity.

Electrophoretic mobility shift assay

Preparation of nuclear extracts and EMSA analysis were performed as described by Jeong *et al*.[30] Briefly, RAW264.7 cells (1×10^6 cells/100-mm dish) were adapted for 12 h; pretreated with BSO, NAC, or GSH for 2 days; and then stimulated with 300 ng/ml RANKL for 20 min. After washing with ice-cold PBS, nuclear extracts were prepared. EMSA analysis was performed with nuclear extracts and specific double-stranded oligonucleotides containing the consensus DNA-binding site (underlined) for either NF-κB or AP-1 purchased from Santa Cruz Biotechnology: NF-κB, 5′-AGTTGAGGGGACTTTCCCAGGC-3′; mutant NF-κB, 5′-AGTT-GAGGCGACTTTCCCAGGC-3′; AP-1, 5′-CGCTTGATGACTCAGCCGG AA-3′; mutant AP-1, 5′-CGCTTGATGACTTGGCCGGAA-3′. After nuclear extract proteins had reacted with the ^{32}P-labeled oligonucleotide, DNA–protein complexes were separated from free oligonucleotides on a native 5% polyacrylamide gel in 0.5 × Tris-borate/EDTA buffer. The gels were then dried and photographed.

Immunoblot and confocal microscopic analyses

Nuclear and cytosolic fractions from RAW264.7. cells exposed to various conditions were prepared as described previously.[30] A lysis buffer (50 mM Tris-HCl, pH 7.4, 150 mM NaCl, 1 mM EDTA, 1% Nonidet P-40, 0.1% SDS, and 1 × protease inhibitor cocktail) was used to obtain whole-cell lysates from intact cells. The samples were fractionated by 10% SDS-polyacrylamide gel electrophoresis and the separated proteins were blotted onto an Immobilon-P membrane (Millipore). Probing was with rabbit antibodies to MAPKs (ERK, phospho-ERK, JNK, phospho-JNK, p38, and phospho-p38; Cell Signaling), IkBα (Cell Signaling), p65 (for NF-κB), c-Jun (for AP-1, Santa Cruz Biotechnology), and β-actin (Sigma) as well as mouse antibodies to TFIIB (BD Biosciences). All blots were overlaid with appropriate HRP-conjugated secondary antibodies and developed by ECL.

For confocal microscopy,[31] RAW264.7 cells were seeded on glass coverslips and cultured in α-MEM media containing BSO, NAC, or GSH for 2 days. Cells were then stimulated with RANKL (300 ng/ml) for 20 min, fixed with 3.7% paraformamide at room temperature, and permeabilized with 0.5% (w/v) saponin. After washing with PBS and blocking with PBS containing 4% sheep serum for 30 min, cells were incubated with rabbit antibodies to p65 (100:1) and to c-Jun (500:1) for 1 h and stained with FITC-conjugated sheep anti-rabbit IgG (Sigma). Nuclei were counter-stained with DAPI, and the images were analyzed under an LSM510 meta confocal microscope (Carl Zeiss).

Cell proliferation and viability

Cell proliferation and viability after exposure to various conditions were determined by trypan blue exclusion assessment as reported by Jeong *et al*.[32]

Free thiol quantification

Intracellular thiol contents of cytosolic extracts were determined using both DTNB exposure and optical density measurements at 412 nm as described previously.[33] GSH was used as the calibration standard.

Bone resorption assay

BMMs (3×10^4 cells/1 ml/well) were seeded in 24-well OAAS plates (Osteogenic Core Technologies, Korea) and cultured as described in the OC differentiation section. After the formation of mature OCs in the presence of M-CSF and RANKL, the cells were further cultured with or without BSO for 2 days. Then, the OAAS plates were treated with 5% sodium hypochlorite for 5 min, washed with distilled water, and air-dried. The resorption area was photographed through a light microscope and calculated using Image-Pro Plus version 4.5 (Media Cybernetics).

Acknowledgements

This study was supported by grant number 01-PJ5-PG1-01CH12-0002 from the Korea Health 21 R&D Project, Ministry of Health & Welfare, Republic of Korea (B-M Min).

References

1. Stadtman ER (1992) Protein oxidation and aging. Science 257: 1220–1224
2. Rossi R, Milzani A, Dalle-Donne I, Giustarini D, Lusini L, Colombo R and Di Simplicio P (2002) Blood glutathione disulfide: *in vivo* factor or *in vitro* artifact? Clin. Chem. 48: 742–753
3. Winiarska K, Drozak J, Wegrzynowicz M, Jagielski AK and Bryla J (2003) Relationship between gluconeogenesis and glutathione redox state in rabbit kidney-cortex tubules. Metabolism 52: 739–746
4. Hansen JM, Carney EW and Harris C (2001) Altered differentiation in rat and rabbit limb bud micromass cultures by glutathione modulating agents. Free Radic. Biol. Med. 31: 1582–1592
5. Schafer FQ and Buettner GR (2001) Redox environment of the cell as viewed through the redox state of the glutathione disulfide/glutathione couple. Free Radic. Biol. Med. 30: 1191–1212
6. Lu SC (1999) Regulation of hepatic glutathione synthesis: current concepts and controversies. FASEB J. 13: 1169–1183
7. Cotgreave IA and Gerdes RG (1998) Recent trends in glutathione biochemistry – glutathione–protein interactions: a molecular link between oxidative stress and cell proliferation? Biochem. Biophys. Res. Commun. 242: 1–9
8. Darden AG, Ries WL, Wolf WC, Rodriguiz RM and Key Jr LL (1996) Osteoclastic superoxide production and bone resorption: stimulation and inhibition by modulators of NADPH oxidase. J. Bone Miner. Res. 11: 671–675
9. Yang S, Madyastha P, Bingel S, Ries W and Key L (2001) A new superoxide-generating oxidase in murine osteoclasts. J. Biol. Chem. 276: 5452–5458
10. Fraser JH, Helfrich MH, Wallace HM and Ralston SH (1996) Hydrogen peroxide, but not superoxide, stimulates bone resorption in mouse calvariae. Bone 19: 223–226
11. Yang S, Ries WL and Key Jr LL (1998) Nicotinamide adenine dinucleotide phosphate oxidase in the formation of superoxide in osteoclasts. Calcif. Tissue Int. 63: 346–350
12. Suda T, Takahashi N, Udagawa N, Jimi E, Gillespie MT and Martin TJ (1999) Modulation of osteoclast differentiation and function by the new members of the tumor necrosis factor receptor and ligand families. Endocr. Rev. 20: 345–357
13. Pfaff M and Jurdic P (2001) Podosomes in osteoclast-like cells: structural analysis and cooperative roles of paxillin, proline-rich tyrosine kinase 2 (Pyk2) and integrin $\alpha v\beta 3$. J. Cell Sci. 114: 2775–2786
14. Teitelbaum SL and Ross FP (2003) Genetic regulation of osteoclast development and function. Nat. Rev. Genet. 4: 638–649
15. Boyle WJ, Simonet WS and Lacey DL (2003) Osteoclast differentiation and activation. Nature 423: 337–342
16. Tian L, Shi MM and Forman HJ (1997) Increased transcription of the regulatory subunit of gamma-glutamylcysteine synthetase in rat lung epithelial L2 cells exposed to oxidative stress or glutathione depletion. Arch. Biochem. Biophys. 342: 126–133
17. Lean JM, Davies JT, Fuller K, Jagger CJ, Kirstein B, Partington GA, Urry ZL and Chambers TJ (2003) A crucial role for thiol antioxidants in estrogen-deficiency bone loss. J. Clin. Invest. 112: 915–923
18. Hotokezaka H, Sakai E, Kanaoka K, Saito K, Matsuo K, Kitaura H, Yoshida N and Nakayama K (2002) U0126 and PD98059, specific inhibitors of MEK, accelerate differentiation of RAW264.7 cells into osteoclast-like cells. J. Biol. Chem. 277: 47366–47372
19. Flohe L, Brigelius-Flohe R, Saliou C, Traber MG and Packer L (1997) Redox regulation of NF-kB activation. Free Radic. Biol. Med. 22: 1115–1126
20. Sen CK and Packer L (1996) Antioxidant and redox regulation of gene transcription. FASEB J. 10: 709–720
21. Sun Y and Oberley LW (1996) Redox regulation of transcriptional activators. Free Radic. Biol. Med. 21: 335–348
22. Aw TY (1999) Molecular and cellular responses to oxidative stress and changes in oxidation-reduction imbalance in the intestine. Am. J. Clin. Nutr. 70: 557–565
23. Sauer H, Wartenberg M and Hescheler J (2001) Reactive oxygen species as intracellular messengers during cell growth and differentiation. Cell Physiol. Biochem. 11: 173–186
24. Forman HJ, Fukuto JM and Torres M (2004) Redox signaling: thiol chemistry defines which reactive oxygen and nitrogen species can act as second messengers. Am. J. Physiol. Cell Physiol. 287: C246–256
25. Iotsova V, Caamano J, Loy J, Yang Y, Lewin A and Bravo R (1997) Osteopetrosis in mice lacking NF-kB1 and NF-kB2. Nat. Med. 3: 1285–1289
26. Jimi E, Aoki K, Saito H, D'Acquisto F, May MJ, Nakamura I, Sudo T, Kojima T, Okamoto F, Fukushima H, Okabe K, Ohya K and Ghosh S (2004) Selective inhibition of NF-kB blocks osteoclastogenesis and prevents inflammatory bone destruction *in vivo*. Nat. Med. 10: 617–624
27. Feldmann M, Andreakos E, Smith C, Bondeson J, Yoshimura S, Kiriakidis S, Monaco C, Gasparini C, Sacre S, Lundberg A, Paleolog E, Horwood NJ, Brennan FM and Foxwell BM (2002) Is NF-kB a useful therapeutic target in rheumatoid arthritis? Ann. Rheum. Dis. 61 (Suppl 2): ii13–ii18
28. Wani MR, Fuller K, Kim NS, Choi Y and Chambers T (1999) Prostaglandin E2 cooperates with TRANCE in osteoclast induction from hemopoietic precursors: synergistic activation of differentiation, cell spreading, and fusion. Endocrinology 140: 1927–1935
29. Appleman LJ, van Puijenbroek AA, Shu KM, Nadler LM and Boussiotis VA (2002) CD28 costimulation mediates down-regulation of p27kip1 and cell cycle progression by activation of the PI3K/PKB signaling pathway in primary human T cells. J. Immunol. 168: 2729–2736
30. Jeong DW, Yoo MH, Kim TS, Kim JH and Kim IY (2002) Protection of mice from allergen-induced asthma by selenite: prevention of eosinophil infiltration by inhibition of NF-kB activation. J. Biol. Chem. 277: 17871–17876
31. Howard MJ and Isacke CM (2002) The C-type lectin receptor Endo180 displays internalization and recycling properties distinct from other members of the mannose receptor family. J. Biol. Chem. 277: 32320–32331
32. Jeong D, Kim TS, Chung YW, Lee BJ and Kim IY (2002) Selenoprotein W is a glutathione-dependent antioxidant *in vivo*. FEBS Lett. 517: 225–228
33. Kowaltowski AJ, Vercesi AE and Castilho RF (1997) Mitochondrial membrane protein thiol reactivity with N-ethylmaleimide or mersalyl is modified by Ca^{2+}: correlation with mitochondrial permeability transition. Biochim. Biophys. Acta. 1318: 395–402